

Supplementary material and methods

Electrophysiology

Animals and brain slice preparation

Experiments were performed on brain slices from 4- to 5-week old female and male *Afg3l2*^{PC-KO} mice and their control littermates. Animals were anesthetized with halothane (B4388; Sigma-Aldrich) and subsequently decapitated. The brain was rapidly removed and the cerebellum was immediately dissected. Sagittal slices (250 – 300 μm) of the cerebellum were cut with a vibration microtome (HM-650 V; Thermo Scientific) under cold (4°C), carbogenated (95% O₂ and 5% CO₂), glycerol-based modified artificial cerebrospinal fluid (GaCSF). GaCSF contained (in mM): 250 Glycerol, 2.5 KCl, 2 MgCl₂, 2 CaCl₂, 1.2 NaH₂PO₄, 10 HEPES, 21 NaHCO₃, 5 Glucose adjusted to pH 7.2 (with NaOH) resulting in an osmolarity of ~310 mOsm. Brain slices were transferred into carbogenated artificial cerebrospinal fluid (aCSF). First, they were kept for 20 min in a 35°C 'recovery bath' and then stored at room temperature (24°C) for at least 30 min prior to recording. aCSF contained (in mM): 125 NaCl, 2.5 KCl, 2 MgCl₂, 2 CaCl₂, 1.2 NaH₂PO₄, 21 NaHCO₃, 10 HEPES, and 5 Glucose adjusted to pH 7.2 (with NaOH) resulting in an osmolarity of ~310 mOsm. Slices were transferred to a recording chamber (~3 ml volume) and continuously superfused with carbogenated aCSF at a flow rate of ~2 ml·min⁻¹. Experiments were carried out at ~32°C using an inline solution heater (SH27B; Warner Instruments) operated by a temperature controller (TC-324B; Warner Instruments). Neurons in the cerebellum were visualized with a fixed-stage upright microscope (BX51WI; Olympus), using a 60x water immersion objective (LUMplan FI/IR; 60 \times ; 0.9 numerical aperture; 2 mm working distance; Olympus) with infrared-differential interference contrast (1). PCs were identified by the anatomical location in the cerebellum and by their YFP fluorescence using a Chroma 41001 filter set (excitation, HQ480/40; beam splitter, Q505LP; emission, HQ535/50 m; Chroma). Current-clamp

recordings were performed with an EPC9 patch-clamp amplifier (HEKA) controlled by the PatchMaster software (version 2.32; HEKA). Data were sampled at intervals of 10 μ s (100 kHz) with a CED 1401 using Spike2 (both Cambridge Electronics). The liquid junction potential between intracellular and extracellular solution was compensated (14.6 mV; calculated with Patcher's Power Tools plug-in for Igor Pro 6 [Wavemetrics]).

Perforated patch recordings

Perforated patch recordings were performed using protocols modified from Horn & Marty (2) and Akaike & Harata (3). Electrodes with tip resistances between 3 and 5 MOhm were fashioned from borosilicate glass (0.86 mm inner diameter; 1.5 mm outer diameter; GB150-8P; Science Products) with a vertical pipette puller (PP-830; Narishige). Patch recordings were performed with ATP and GTP free pipette solution containing (in mM): 128 K-gluconate, 10 KCl, 10 HEPES, 0.1 EGTA, 2 MgCl₂ and adjusted to pH 7.3 (with KOH) resulting in an osmolarity of \sim 300 mOsm. ATP and GTP were omitted from the intracellular solution to prevent uncontrolled permeabilization of the cell membrane (4). The patch pipette was tip filled with internal solution and back filled with 0.02% tetraethylrhodamine-dextran (D3308, Invitrogen) and amphotericin-containing internal solution (\sim 200-250 μ g \cdot ml⁻¹; G4888; Sigma) to achieve perforated patch recordings. Amphotericin was dissolved in dimethyl sulfoxide (final concentration: 0.1- 0.3%; DMSO; D8418, Sigma) as described previously (5); and was added to the modified pipette solution shortly before use. The used DMSO concentration had no obvious effect on the investigated neurons. During the perforation process access resistance (R_a) was constantly monitored and experiments were started after R_a and the action potential (AP) amplitude were stable (\sim 15 – 20 min). A change to the whole-cell configuration was indicated by diffusion of tetraethylrhodamine-dextran into the neuron. Such experiments were rejected. For each recording the firing rate was determined by

averaging the frequency over 2 minutes as after the perforation was stable. The cell input resistance was calculated from voltage responses to small hyperpolarizing current pulses.

Data analysis

Data analysis was performed with Spike2 (Cambridge Electronics), Graphpad Prism (version 5.0b; Graphpad Software Inc) and Igor Pro. Numerical values in the text are given as mean \pm standard error. Two-tailed unpaired *t* tests were performed to determine differences in electrophysiological properties between PCs of *Afg3l2*^{PC-KO} mice and PCs of control littermates. A significance level of 0.05 was accepted for all tests.

Single-cell labeling

To label single cells, 1% biocytin (B4261, Sigma) was added to the pipette solution. After the recordings, the brain slices were fixed in Roti-Histofix (P0873, Carl Roth) for ~12 h at 4°C and rinsed in 0.1 M PBS buffered solution (PBS; pH 7.2, 3 times for 10 min each time). Brain slices were incubated in PBS containing 1% Triton X-100 and 10% normal goat serum (30 min, RT; Serva). Afterwards, the slices were incubated in Alexa Fluor 633 (Alexa 633)-conjugated streptavidin (1:600, 2h, RT; S21375, Molecular Probes) that was dissolved in PBS containing 10% normal goat serum (S-1000, Vector Labs). Brains were rinsed in PBS (5 times for 10 min each time, RT), dehydrated, cleared, and mounted in methylsalicylate (M6752, Sigma-Aldrich). Fluorescence images of brain slices were captured with a confocal microscope (LSM 510, Carl Zeiss) equipped with Plan-Neofluar \times 10 (0.3 NA), Plan-Apochromat \times 20 (0.75 NA), and Plan-Apochromat \times 63 (1.4 NA Oil) objectives. Streptavidin-Alexa 633 was excited with a He-Ne Laser at 633 nm, and emission was collected through a 650-nm LP filter. Scaling, contrast enhancement, and *z*-projections were performed with ImageJ v1.35d and the WCIF plug-in bundle (www.uhnresearch.ca/facilities/wcif/). The final figures were prepared with Photoshop and Illustrator CS5 (Adobe Systems)

Mitochondrial translation assay in MEFs

MEFs were washed twice with Met/Cys free media for 10 min. Cytosolic translation was blocked using cyclohexamide and emetine for 15 min. CCCP (20 μ M) was added for 5 or 10 min as indicated and the control sample was treated with equal volume of ethanol for 10 min. To label mtDNA encoded peptides cells were incubated with 150 μ Ci [³⁵S]-Met/Cys/ml (Hartmann Analytic) for 30 min followed by two washing steps with cold growth media and three times with cold PBS.

BN-PAGE

BN-PAGE was performed essentially as previously described (6).

Supplementary References

1. Dodt HU. Infrared-interference videomicroscopy of living brain slices. *Adv Exp Med Biol.* 1993;333:245-249.
2. Horn R, and Marty A. Muscarinic activation of ionic currents measured by a new whole-cell recording method. *J Gen Physiol.* 1988;92(2):145-159.
3. Akaike N, and Harata N. Nystatin perforated patch recording and its applications to analyses of intracellular mechanisms. *Jpn J Physiol.* 1994;44(5):433-473.
4. Lindau M, and Fernandez JM. A patch-clamp study of histamine-secreting cells. *J Gen Physiol.* 1986;88(3):349-368.
5. Kyrozis A, and Reichling DB. Perforated-patch recording with gramicidin avoids artifactual changes in intracellular chloride concentration. *J Neurosci Methods.* 1995;57(1):27-35.
6. Wittig I, Braun HP, and Schagger H. Blue native PAGE. *Nature protocols.* 2006;1(1):418-428.

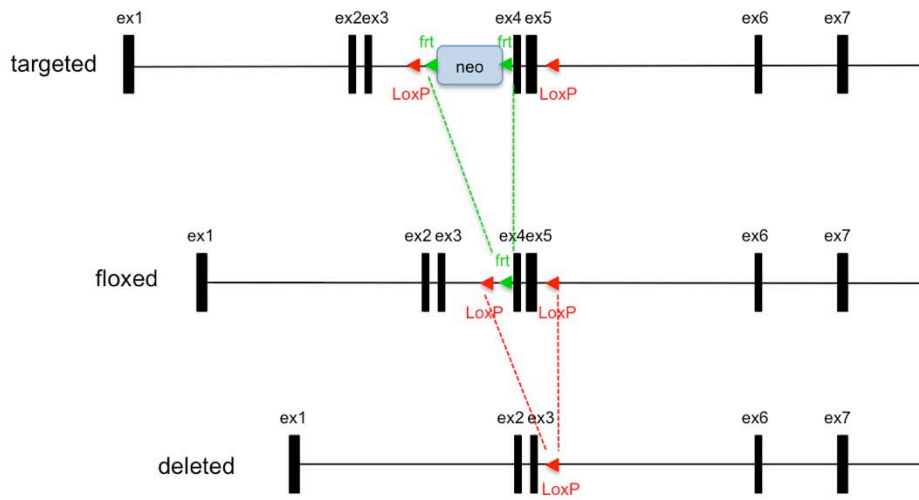


Figure S1. Design of *Afg3l2* conditional mouse model

On the top is shown a schematic representation of the targeted *Afg3l2* locus. Upon Flp-mediated recombination the floxed allele is obtained (middle). This contains two LoxP sites flanking exons 4 and 5. Cre-mediated recombination generates a deletion of exons 4 and 5 (bottom).

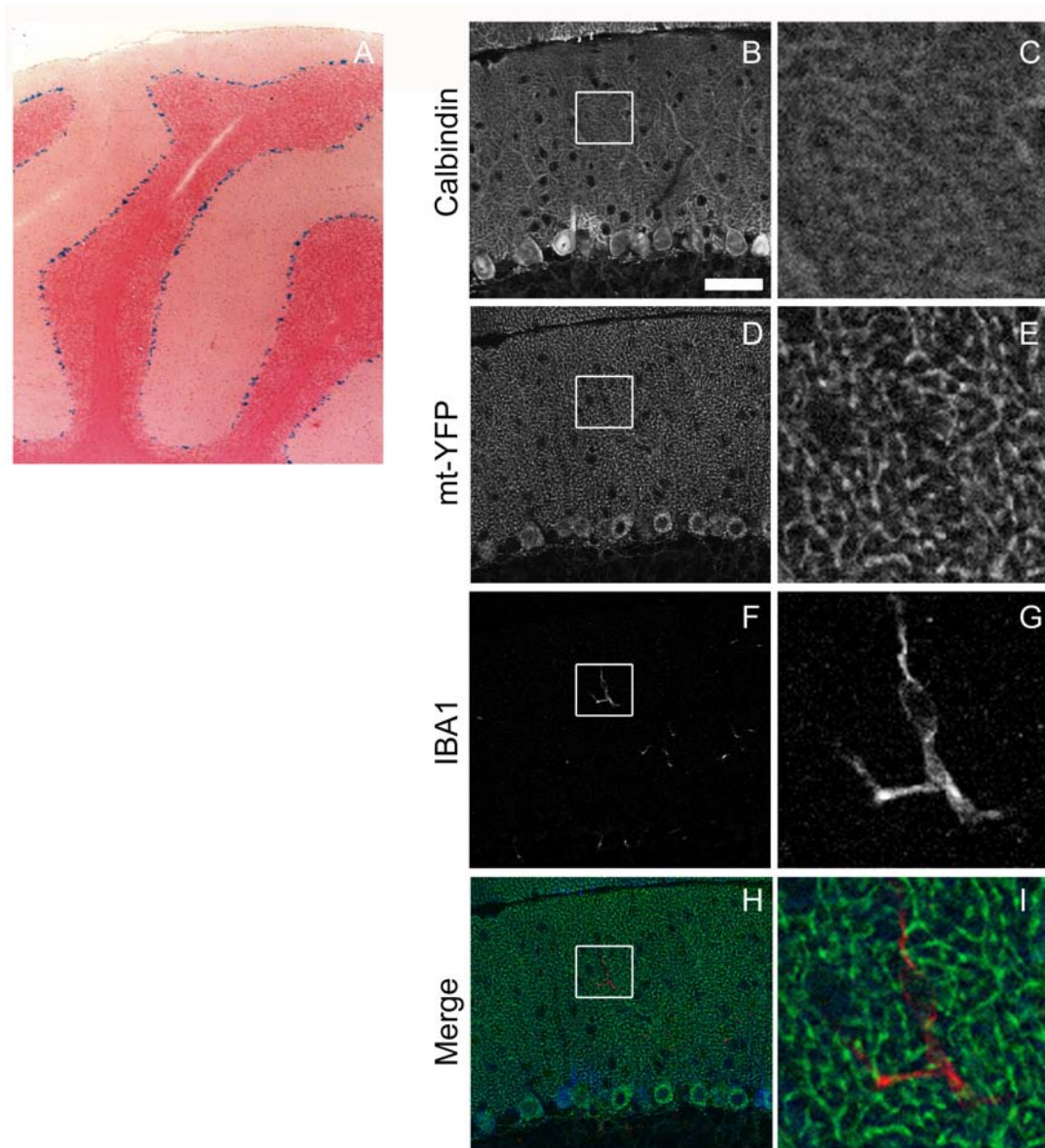


Figure S2. Cre recombinase is specifically expressed in PCs in L7-Cre transgenic mice

(A) L7-Cre transgenic mice were crossed with a strain expressing β -galactosidase under the ROSA26 promoter. Only PCs appear blue in the cerebellum. (B-I) The cerebellum of L7-Cre; ROSA26^{+7/SmY} transgenic mice was analyzed for mitochondrial YFP expression. PCs are decorated using an antibody against calbindin (B, enlarged box in C), the mitochondrial network is labeled with mito-YFP (D, enlarged box in E), and IBA1 antibody is used to mark microglia (F, enlarged box in G). In merged images (H, I) pseudocolors were used: calbindin is in blue, mito-YFP is green and microglia is red. The labeled mitochondrial network fills the PC dendrites but shows no colocalization with microglia. Scale bar: 50 μ m.

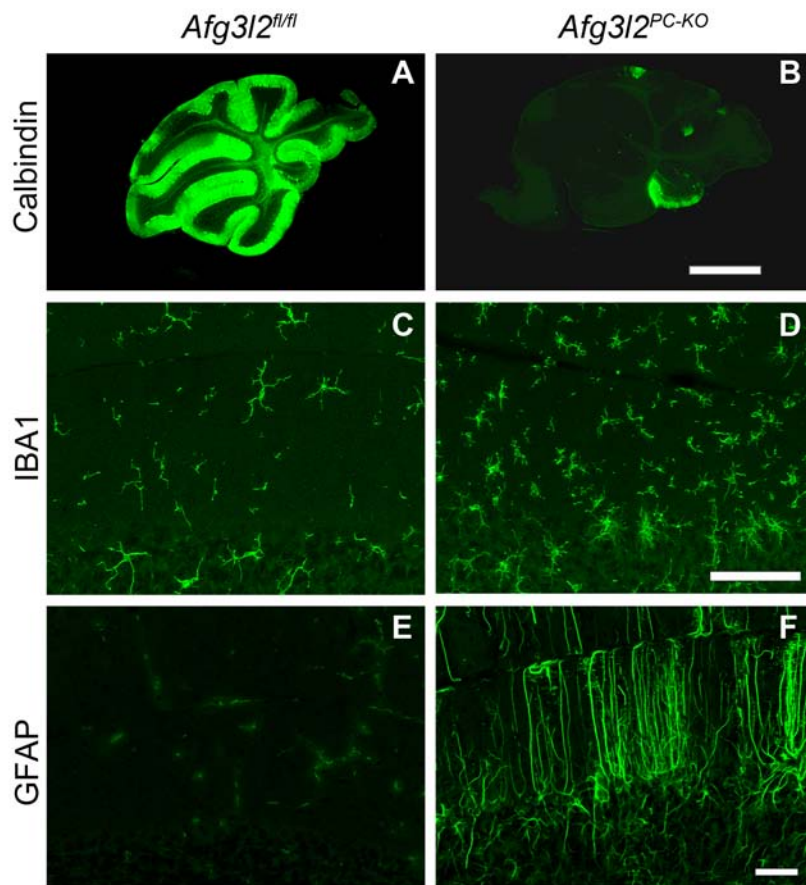


Figure S3. Few PCs survive in 12 weeks old *Afg3l2^{PC-KO}* mice. Vibratome sections of the cerebellum at 12 weeks from *Afg3l2^{fl/fl}* and *Afg3l2^{PC-KO}* mice and stained for calbindin (A, B) to show PC loss, IBA1 (C, D) to detect resting and activated microglia, and GFAP (E, F) to mark reactive astrocytes. Scale bars: 200 μm (A, B), 50 μm (C, D), 100 μm (E, F).

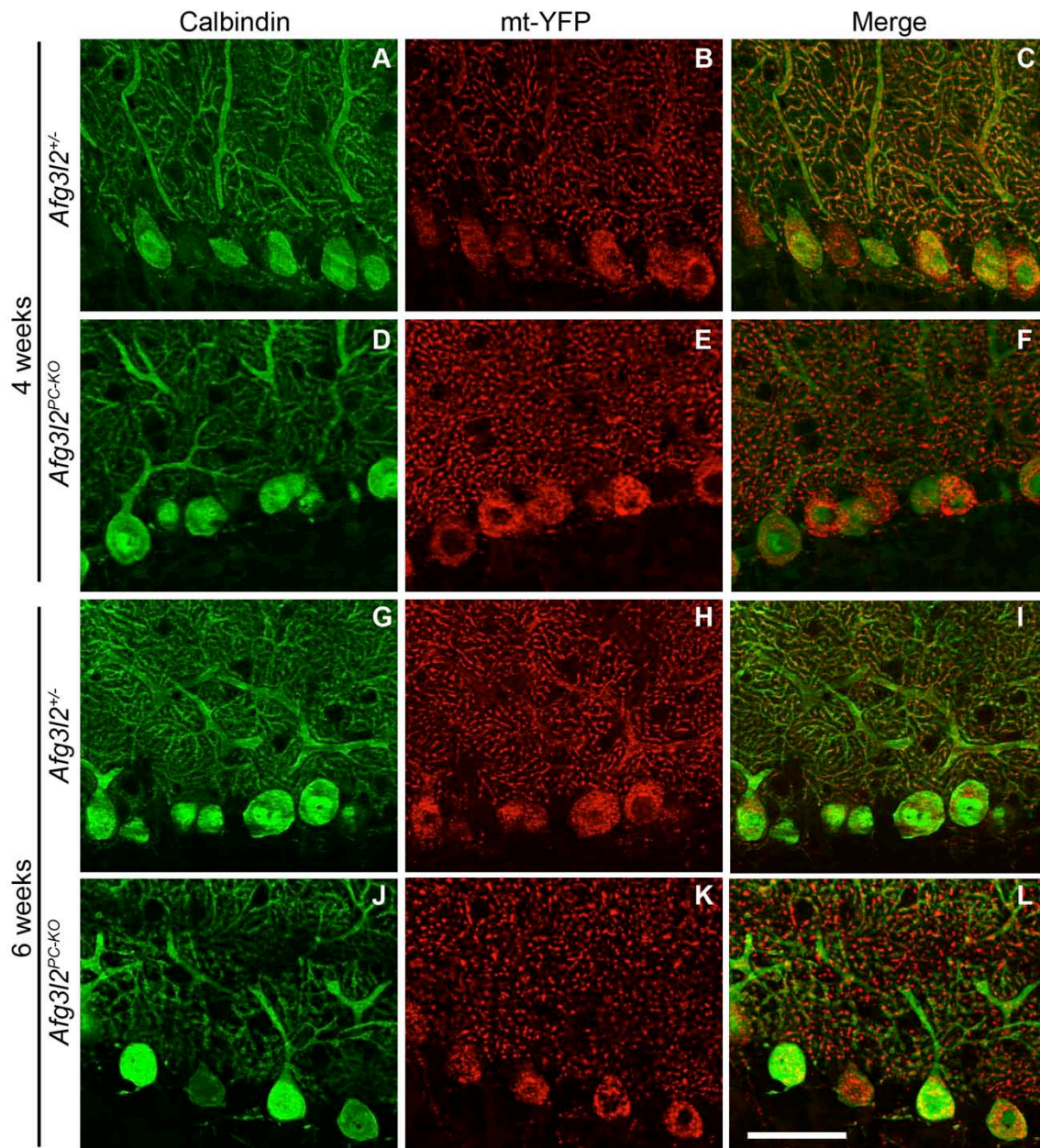


Figure S4. Evolution of mitochondrial morphology phenotype in *Afg312*^{PC-KO} mice.

The mitochondrial network is labeled with mt-YFP (B, E, H, K), while PC dendrites are decorated using an antibody against calbindin (A, D, G, J). In merged images (C, F, I, L) pseudocolors were used: calbindin is in green, while mt-YFP is in red. mt-YFP expression in control mice at 4 and 6 weeks of age shows an elongated network of mitochondria (B, H) that follows the pattern of PC dendrites labeled with calbindin (A, C, G, I). In 4 weeks old *Afg312*^{PC-KO} mice, the mitochondrial network shows initial signs of fragmentation (E, F). At 6 weeks, *Afg312*^{PC-KO} mice display severe fragmentation of the mitochondrial network (K, L). Scale bar 50 μ m.

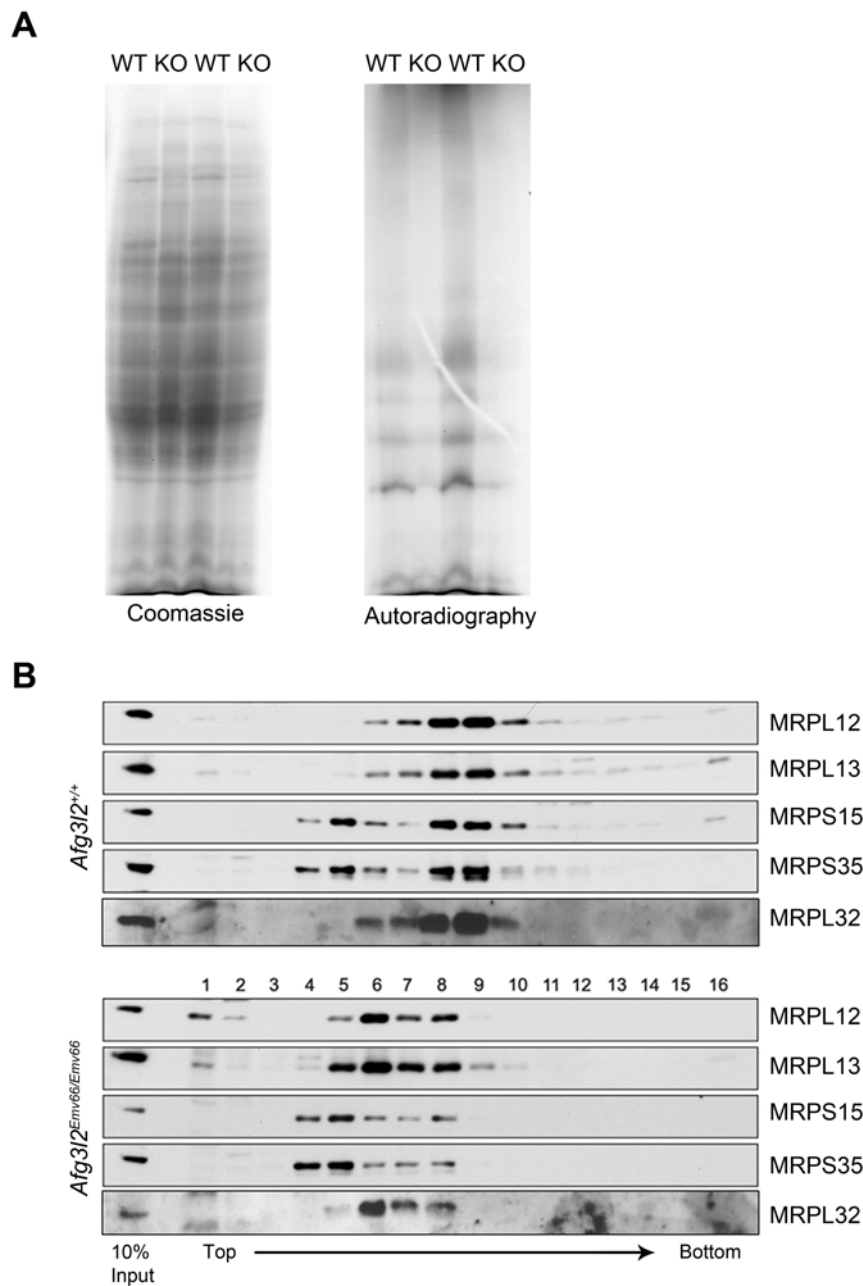


Figure S5. Impaired mitochondrial protein synthesis and mitoribosome assembly in liver mitochondria from *Afg3l2*^{Emv66/Emv66} mice.

(A) *In organello* translation after labeling with ³⁵S-Met shows reduced *de novo* synthesized protein levels in the liver of *Afg3l2*^{Emv66/Emv66} (KO) mice compared with *Afg3l2*^{+/+} mice (WT). Coomassie brilliant blue staining of the gel shows equal loading of proteins. (B) Mitochondrial ribosome profile shows a clear shift to less dense fractions in the pattern of large ribosomal subunits in liver mitochondria of *Afg3l2*^{Emv66/Emv66} when compared to the control *Afg3l2*^{+/+} mice, and reduced levels of assembled mitoribosomes.

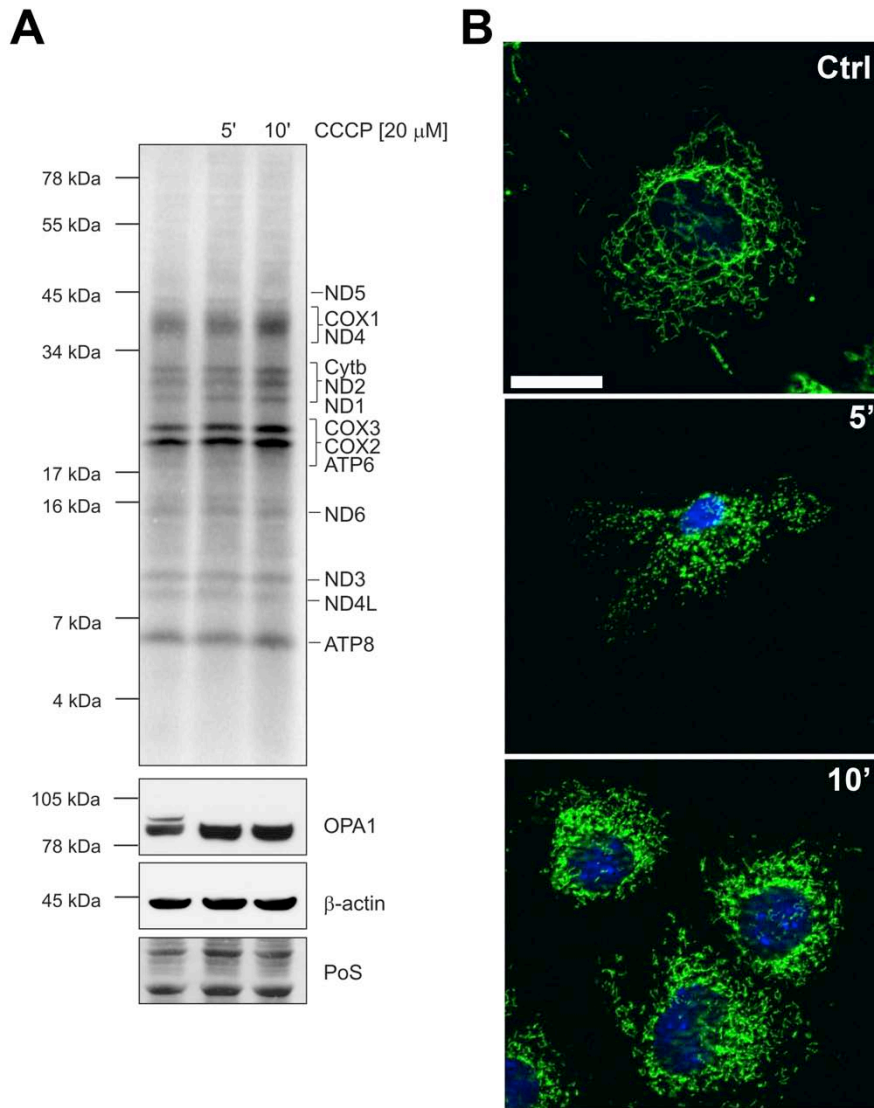


Figure S6. Fragmentation of mitochondrial network does not affect mitochondrial protein synthesis

(A) In vivo labeling of newly synthesized mitochondrial encoded proteins with 35 S-Met shows no difference between control MEFs and cells treated for 5 min or 10 min with CCCP in order to induce fragmentation of the mitochondrial network. OPA1 long isoforms are lost after CCCP treatment. β -actin and Ponceau S were used as loading control. (B) Representative images of the mitochondrial network of the cells used for the experiment. The mitochondrial network is visualized using an anti-Tom20 antibody (green) and the nuclei are stained with DAPI (blue). Control MEFs (Ctrl) show a tubular mitochondrial network, while cells treated with CCCP for 5 or 10 min display a fragmented mitochondrial network. Scale bar 20 μ m.

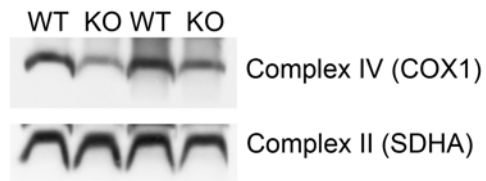


Figure S7. Reduced assembly of respiratory complex IV in *Afg3l2*^{Emv66/Emv66} mice

Blue native analysis using digitonin (6g/g) as detergent shows decreased levels of assembled complex IV in the brain of *Afg3l2*^{Emv66/Emv66} mice. Complex II (SDHA) was used as loading control.